# Photochemistry of 4′-Benzophenone-Substituted Nucleoside Derivatives as Models for Ribonucleotide Reductases: Competing Generation of 3′-Radicals and Photoenols

Thomas E. Lehmann,[†] Gerhard Müller,[†] and Albrecht Berkessel*[,‡]

*Institut für Organische Chemie der Universität zu Köln, Greinstr. 4, 50939 Köln, Germany, and Bayer AG, Central Research, ZF-WF, Building Q 18, 51368 Leverkusen, Germany*

*Received November 23, 1999*

Ribonucleotide reductases (RNRs) catalyze the 2′-reduction of ribonucleotides, thus providing 2′-deoxyribonucleotides, the monomers for DNA-biosynthesis. The current mechanistic hypothesis for the catalysis effected by this class of enzymes involves a sequence of radical reactions. A 3′-hydrogen abstraction, effected by a radical at the enzyme's active site, is believed to initiate the catalytic cycle. As models for this substrate−enzyme interaction, the photochemically induced intramolecular hydrogen abstraction in a series of 4′-benzophenone-substituted nucleoside analogues was studied. Model compounds with hydroxy-, methoxy-, mesyloxy-groups or a cyclic carbonate in 2′- and 3′-positions were investigated. Depending on the substitution pattern, two different types of photoproducts were observed: Those which result from photoenol formation ($\gamma$-H-abstraction) and those which result from abstraction of the 3′-H-atom ($\delta$-H-abstraction). Photoenol formation was further supported by H/D-exchange experiments. Thus, the 3′-H-abstraction postulated as the initial step in RNR action was successfully modeled by photolysis of 4′-benzophenone-substituted nucleoside analogues. The regioselectivity of the photochemical H-abstraction and thus of the product distribution as a function of the 2′- and 3′-substituents was rationalized on the basis of a conformational analysis of the four model systems, utilizing molecular mechanics simulations.

## Introduction

In all known organisms, 2′-deoxyribonucleotides are synthesized by 2′-reduction of ribonucleotides. This deoxygenation (eq 1) is effected by ribonucleotide reductases (RNRs).[1]

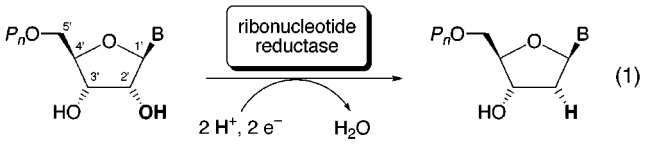


Therefore, RNRs play a central role in DNA biosynthesis and in cell division, and they are potential drug targets for tumor and viral diseases.[2] A radical reaction mechanism has been proposed for the action of ribonucleotide reductases.[3] In this mechanistic proposal, the catalytic cycle is initiated by the regioselective attack of a radical species X• in the enzyme's active site on the 3′-position of the substrate nucleotide. As a result, the 3′-hydrogen atom is homolytically removed and the so-called "3′-radical" **A** (Scheme 1) is generated. This proposed mechanism of catalysis is based on studies with isotopically labeled substrates and substrate analogues, as well as on the investigation of enzymes modified by site-directed mutagenesis.[4−6] Most importantly, at least

**Scheme 1. Design of Model Compounds**

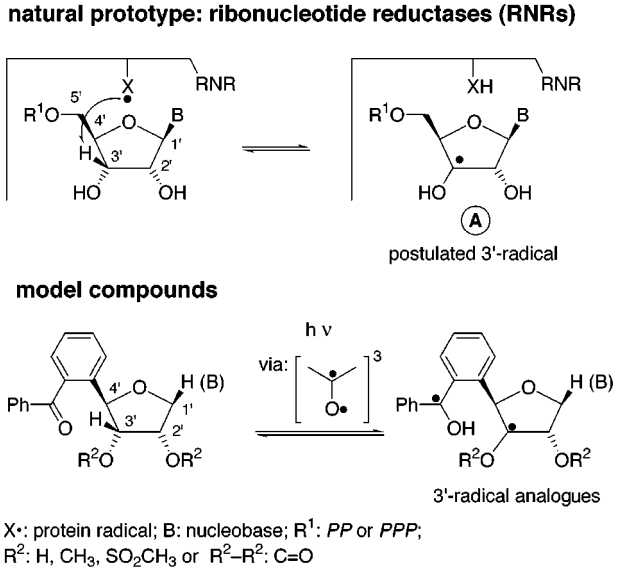


* To whom correspondence should be addressed. Phone: int+49-221-470-3283. Fax: int+49-221-470-5102. e-mail: berkessel@uni-koeln.de.

† Bayer AG.

‡ Institut für Organische Chemie der Universität zu Köln.

(1) For reviews see: (a) Stubbe, J. *Proc. Natl. Acad. Sci. U.S.A.* **1998**, *95*, 2723. (b) Jordan, A.; Reichard, P. *Annu. Rev. Biochem.* **1998**, *67*, 71. (c) Sjöberg, B.-M. *Struct. Bonding (Berlin)* **1997**, *88*, 139. (d) Reichard, P. *Science* **1993**, *260*, 1773. (e) Stubbe, J. *Adv. Enzymol. Relat. Areas Mol. Biol.* **1990**, *63*, 349.

(2) (a) Stubbe, J.; van der Donk, W. A. *Chem. Biol.* **1995**, *2*, 793. (b) *Inhibitors of Ribonucleoside Diphosphate Reductase Activity*; International Encyclopedia of Pharmacology and Therapeutics, Section 128; Cory, J. G., Cory, A. H., Eds., Pergamon Press: New York, 1989.

(3) (a) Licht, S.; Gerfen, G. J.; Stubbe, J. *Science* **1996**, *271*, 477. (b) Stubbe, J. *J. Biol. Chem.* **1990**, *265*, 5329. (c) Reichard, P.; Ehrenberg, A. *Science* **1983**, *221*, 514. (d) Stubbe, J.; Ator, M., Krenitsky, T. *J. Biol. Chem.* **1983**, *258*, 1625 and ref 1b.

(4) (a) Stubbe, J.; Ackles, D. *J. Biol. Chem.* **1980**, *255*, 8027 and ref 3d. For reviews of early literature, see: (b) Thelander, L.; Reichard, P. *Annu. Rev. Biochem.* **1979**, *48*, 133. (c) Follmann, H. *Angew. Chem., Int. Ed. Engl.* **1974**, *13*, 569 (d) Hogenkamp, H. P. C.; Sando, G. N. *Struct. Bonding (Berlin)* **1974**, *20*, 23.

(5) (a) Salowe, S.; Bollinger, J. M.; Ator, M.; Stubbe, J.; McCracken, J.; Peisach, J.; Samano, M. C.; Robins, M. J. *Biochemistry* **1993**, *32*, 12749. (b) Salowe, S. P.; Ator, M. A.; Stubbe, J. *Biochemisty* **1987**, *26*, 3408. (c) Ator, M. A.; Stubbe, J. *Biochemistry* **1985**, *24*, 7214. (d) Ator, M.; Salowe, S. P.; Stubbe, J.; Emptage, M. H.; Robins, M. J. *J. Am. Chem. Soc.* **1984**, *106*, 1886. (e) Sjöberg, B.-M.; Gräslund, A.; Eckstein, F. *J. Biol. Chem.* **1983**, *258*, 8060. (f) Thelander, L.; Larsson, B.; Hobbs, J.; Eckstein, F. *J. Biol. Chem.* **1976**, *251*, 1398 and ref 1b.

10.1021/jo991811s CCC: $19.00 
Published on Web 03/23/2000

one of the three classes of RNRs is known to harbor a stable tyrosyl radical.[7] Finally, the X-ray crystal structures of the two protein subunits (R1 and R2) of *Escherichia coli* RNR support the idea of a radical deoxygenation sequence, with a cysteine-centered thiyl radical acting as the radical X• in the enzyme's active site.[8]

In an elegant study, Giese et al. recently succeeded in generating the 3′-radical of adenosine by the photoinduced homolytic cleavage of selenol esters.[9a] Most interestingly, they could show that this radical eliminates the 2′-hydroxyl group in a (general) base-catalyzed process.[9a] Of course, the generation of the 3′-radical by homolytic abstraction of the 3′-H-atom would model the natural system much more closely.[9b]

Carbonyl compounds, and in particular benzophenones, are able to initiate reversible homolytic hydrogen abstractions upon photochemical excitation into their triplet states.[10] Therefore, nucleoside analogues were designed which incorporate a benzophenone substituent into the sugar moiety (Scheme 1).[11] With the carbonyl oxygen atom of the benzophenone moiety being fixed near the 3′-hydrogen atom, these model compounds are expected to generate 3′-radicals upon irradiation. Molecular models suggest the attachment of the benzophenone substructure to the 4′-position of the ribose ring (for the sake of clarity, the conventional numbering of the ribose unit in nucleosides is maintained throughout the text). In this arrangement, the carbonyl oxygen atom should be at a favorable distance to the 3′-hydrogen atom. For the first series of photochemical studies, a simplified model system was designed, where the nucleobase was replaced by a hydrogen atom. To test the influence of the substituents at the 2′- and 3′-positions, the four model compounds **1**−**4** were designed. The stereoselective synthesis of **1**−**4** from L-rhamnose was described by us before.[11]

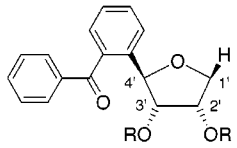


**1**: R = H
**2**: R–R = C=O
**3**: R = $CH_3$
**4**: R = $SO_2CH_3$

In this article, we report the photochemistry of the model compounds **1**−**4**. As it turned out, competing 3′- and 4′-H-abstraction could be observed. Their relative distribution was rationalized by computational analysis of the conformational behavior of the models **1**−**4**.

## Results

**Photolyses of the Model Compounds 1−4. Structures of the Photoproducts.** The photolysis of the model compounds **1**−**4** was carried out in a Rayonet Photoreactor at 350 nm in water-cooled reaction vessels. Generally, 0.6−1.0 mM solutions of **1**−**4** in anhydrous, degassed benzene or acetonitrile were used. Reactions were monitored by HPLC and allowed to proceed to 90−100% conversion, depending on the photochemical stability of the reaction products formed. For the $^1$H NMR monitoring of the reactions, the photolyses were carried out in air-cooled NMR tubes using 128−148 mM solutions in deuterated solvents. The reaction products were usually isolated by preparative HPLC.

**Dihydroxy Model Compound 1.** The photolysis of **1** in benzene-$d_6$ was monitored by NMR, indicating a clean conversion to the ketal **5**. The estimated yield by NMR was 70%, preparative HPLC afforded 31% of pure **5** (eq 2). The structure of **5** was assigned by $^1$H, $^{13}$C, DEPT,[12] DQF-H,H-COSY,[13] JS-ROESYNMR experiments,[14] as well as IR and HRMS spectra.[15a] The interatomic distances obtained from the integration of the ROE signals are in good agreement with those of a molecular model of **5** after minimization in a MM2 force field.[15b]

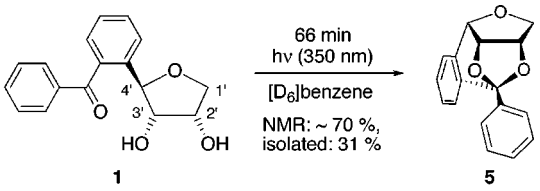


**1** **5** (2)

To clarify the mechanism by which **5** is formed, monodeuterated acetic acid ($CH_3CO_2D$) was added to **1** in benzene-$d_6$. $^1$H NMR monitoring of the photolytic conversion **1** → **5** showed the incorporation of ca. 45% $^2$H in the benzylic position of **5** (eq 3). The incorporation of deuterium was indicated by the reduced integrals of the corresponding proton signals, as well as the observation of the typical coupling patterns at the neighboring protons, imposed by the $I = 1$ nucleus.[15c]

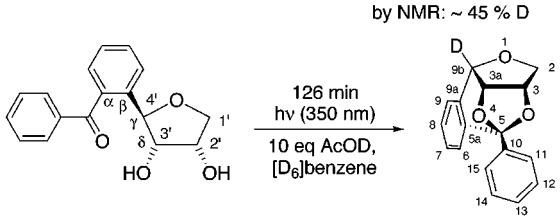


**1** **5** (3)

**Cyclic Carbonate 2.** The cyclic carbonate **2** was rapidly converted upon irradiation in benzene (91% within 10 min). Longer irradiation induced the degradation of the primary photoproducts. After preparative HPLC, 46% of the furan derivative **6** and 9% of the reisolated starting material **2** were obtained. Furthermore, the epimer **7** of the starting material was isolated in a yield of 6% (eq 4).

The structural assignment of the furan derivative **6** rests on $^1$H-, $^{13}$C-, and DEPT-NMR spectra, as well as

(6) (a) Rova, U.; Goodtzova, K.; Ingemarson, R.; Behravan, G.; Gräslund, A.; Thelander, L. *Biochemistry* **1995**, *34*, 4267. (b) Mao, S. S.; Holler, T. P.; Yu, G. X.; Bollinger, J. M.; Booker, S.; Johnston, M. I.; Stubbe, J. *Biochemistry* **1992**, *31*, 9733.(b) Larsson, A.; Sjöberg, B.-M. *EMBO J.* **1986**, *5*, 2037 and ref 1b.

(7) See refs 1a and 6.

(8) (a) Logan, D. T.; Andersson, J.; Sjöberg, B,-M.; Nordlund, P. *Science* **1999**, *283*, 1499. (b) Uhlin, U.; Eklund, H. *Nature* **1994**, *370*, 533. (c) Nordlund, P.; Sjöberg, B.-M.; Eklund, H. *Nature* **1990**, *345*, 593.

(9) (a) Lenz, R.; Giese, B. *J. Am. Chem. Soc.* **1997**, *119*, 2784. For a model study on the related dioldehydratase reaction, see: Müller, P.; Rétey, J. *J. Chem. Soc., Chem. Commun.* **1983**, 1342. (b) Robins, M. J.; Ewing, G. J. *J. Am. Chem. Soc.* **1999**, *121*, 5823.

(10) (a) Wagner, P.; Park, B.-S. In *Organic Photochemistry;* Pawda, A., Ed.; Dekker: New York, 1991; vol. 11, p 227. (b) Wagner, P. J. *Top. Curr. Chem.* **1976**, *66*, 1. (c) Wagner, P. J. *Acc. Chem. Res.* **1971**, *4*, 168.

(11) (a) Lehmann, T. E.; Berkessel, A. *J. Org. Chem.* **1997**, *62*, 302. (b) Lehmann, T. E. *Dissertation*, Universität Heidelberg, 1995.

(12) Doddrell, D. M.; Pegg, D. T.; Bendall, M. R. *J. Magn. Res.* **1982**, *48*, 323.

(13) Piantini, U.; Sørensen, O. W.; Ernst, R. R. *J. Am. Chem. Soc.* **1982**, *104*, 6800.

(14) Schleucher, J.; Quant, S. J.; Glaser, J.; Griesinger, C. *J. Magn. Reson. A* **1995**, *112*, 144.

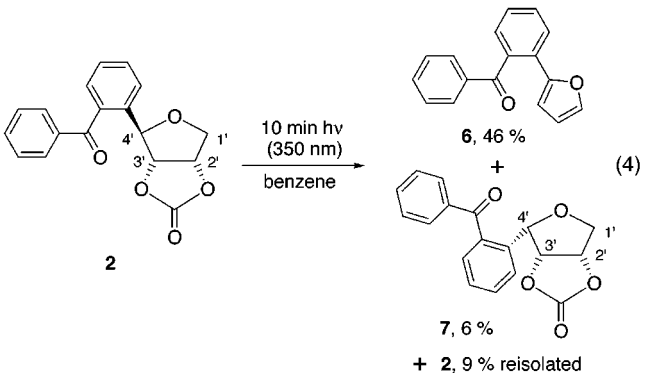


(4)

IR and EI-HRMS. The key spectroscopic features were (a) a very stable [$M^+$] (base peak) in the HRMS for $C_{17}H_{12}O_2$: 248.0861 (calcd 248.0837), (b) the complete absence of any aliphatic CH or C signals in the $^1$H- and $^{13}$C-NMR spectra, (c) the appearance of four new aromatic $^{13}$C-resonances (furane ring), and (d) of bands between 3150 and 3115 cm$^{-1}$ in the IR spectrum, typical of the furanyl C−H stretching vibration.

In compound **7**, only the configuration at the benzylic carbon atom has changed relative to the starting material **2**. As a consequence, the spectral data of **7** are very similar to those of **2**. Nevertheless, an indicative change took place in the coupling constants and the chemical shifts of the aliphatic tetrahydrofuran ring system. For example, the vicinal coupling constant between the benzylic proton and that at C-3′ diminished from 3.5 to 2.6 Hz—as expected for a change from a *trans*- to a *cis*-relationship in 4-substituted tetrahydrofuro[3,4-*d*]dioxolanes.[16]

**Dimethoxy Model Compound 3.** The photolysis of the dimethoxy compound **3** at 350 nm for 40 min resulted in complete conversion (eq 5). The product **8**, which turned out to be stable under the photolysis conditions, could be isolated in 40% yield.[17] NMR monitoring of the reaction in benzene-$d_6$ clearly showed that **8** is indeed the sole major reaction product. When deuterated acetic acid was added, no incorporation of deuterium occurred.

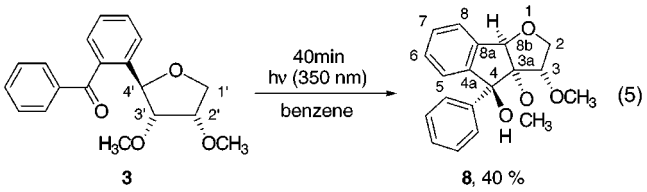


(5)

The constitution of the tricycle **8** was established by $^1$H- and $^{13}$C-DEPT NMR spectra, E.COSY,[18] HMQC,[19] HMBC,[20] and JS-ROESY[14] experiments, as well as EI/CI-MS and IR spectroscopy.[21] The observed ROE-correlations agree very well with the configurations assigned to the newly formed stereogenic centers of **8**. In this respect, the ROE-correlations between the benzylic proton at C-8b and the protons on the convex side of the annulated three-ring system proved particularly indicative.

**Dimesyloxy Model Compound 4.** The irradiation of the dimesyloxy model compound **4** at 350 nm resulted in 96% conversion within ca. 30 min (eq 6). The dimeric product **9** was isolated by preparative HPLC in 16% yield, along with 4% of unchanged starting material. At prolonged irradiation times, decomposition of the primary photoproduct **9** occurred.

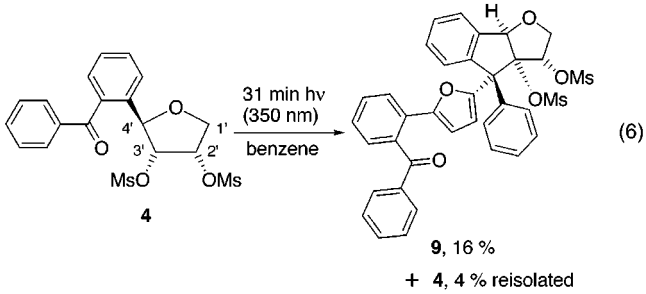


(6)

The structure of **9** was assigned by $^1$H, $^{13}$C-DEPT NMR spectra, E.COSY, HMQC, HMBC, and JS-ROESY experiments as well as EI-/CI-MS and IR spectroscopy.[21] The photoproduct **9** contains the substructures of both the furan **6** and the tricycle **8**. Consequently, the striking similarity of the spectroscopic features of **6**/**8** and **9** is not quite unexpected. Again, the ROE-correlations allowed for the unambiguous assignment of configuration to each stereogenic center of **9**. In the course of the formation of the "dimer" **9** from **4**, 2 equiv of methanesulfonic acid is liberated. HPLC monitoring of the reaction revealed the intermediate formation of the furan **6**, which was not stable in the acidic reaction mixture. The occurrence of new HPLC signals with longer retention times (indicating higher molecular weight and/or increased hydrophobicity) is consistent with the assumption of an acid-catalyzed formation of oligomers from the furan **6**.

**Computational Analysis of the Model Compounds 1−4 by Molecular Modeling.** For the conformational analysis of the compounds **1**−**4** and their corresponding epimers, we followed a bifurcated approach comprising (i) a long-term high-energy molecular dynamics simulation over 1 ns at a temperature of 1000 K, thus enabling the compounds to overcome any barriers on their potential energy hypersurface, and of (ii) a molecular dynamics-based systematic search strategy applied to the dihedral angle encompassing the bond linking the benzophenone with the furanose-C4′ carbon.

(15) (a) The structural alternative of a hemiacetal can be excluded based on the following spectral data: MS: Neither EI-HRMS nor CI-LRMS showed the expected ion at $m/z = 284$; IR: No significant bands in the OH-stretching region. (b) See Supporting Information p S3. (c) As can be seen on p S2 of the Supporting Information, also the signal intensity of the 3′-H-atom decreased by ca. 15%. However, no unambiguous evidence for D-incorporation at the 3′-position could be obtained, e.g., by a change of the coupling pattern of the neighboring 2′-H- as well as the 4′-H-atom.

(16) $^3J$-Coupling constants observed for protons with a *trans*-relationship: 0 Hz = $^3J$ = 2.6 Hz, with a *cis*-relationship: $^3J$ = 3.5 Hz. See Supporting Information p S5 for a complete listing of the coupling constants found for tetrahydrofuro[3, 4-*d*]dioxolanes: six compounds with *trans*- and three with *cis*-oriented 4-substituent.

(17) HPLC monitoring of the reaction showed the formation of a second compound. Preparative HPLC purification of the material showed that the second HPLC signal corresponded to a mixture of two to three side products (9% of starting material by weight) which could not be separated. See also Supporting Information pp S6, S7.

(18) Griesinger, C.; Sørensen, O. W.; Ernst, R. R. *J. Am. Chem. Soc.* **1985**, *107*, 6394.

(19) Bax, A.; Subramanian, S. *J. Magn. Reson. A* **1986**, *67*, 565.

(20) Bax, A.; Summers, M. F. *J. Am. Chem. Soc.* **1986**, *108*, 2093.

(21) For a detailed analysis, please refer to the Experimental Section and the Supporting Information.

The high-energy MD-generated ensemble of conformers allowed for the study of the conformational preferences of all compounds in terms of significantly populated conformational families that were identified by a cluster analysis approach. Due to the high temperature chosen for the production period, more than one distinct conformational family was identified within an energy threshold of a few kcal·mol$^{-1}$ for each compound investigated in this study. Following a cluster analysis approach utilizing a root-mean-square deviation descriptor for pairwise atom-based superposition, two mainly populated conformational families were identified for each compound. Close inspection of representatives of each conformational family revealed a preference for displaying either a short benzophenone C═O−H3′, or a short benzophenone C═O−H4′ distance, respectively, thus clearly corresponding to the outcome of the systematic search simulations described below. For each compound, a C═O−H3′/C═O−H4′ distance−distance plot is deposited in the Supporting Information (p S13). The following discussion of the conformational profiles of each of the investigated compounds is focused on the results obtained from the systematic search protocols employing torsional restraints imposed on a molecular dynamics simulation, since the results obtained are more illustrative and comprehensible when compared to the results of the high-energy molecular dynamics simulations.

The torsion forcing simulation was used to record an energy profile for each compound, describing the energetics for a full rotation around the affected bond. Instead of performing a rigid body rotation, we made preferential use of a molecular dynamics protocol applying an external torque about the specific dihedral angle during the simulation. Thus, the torsion of interest was incremented in 360 distinct steps and harmonically forced to the target values, while the entire molecule was treated as a dynamic entity within its physical force field. This tailored approach allows the molecular systems to remove any intrinsic steric or electronic repulsion, that may be caused by the systematic bond rotation, since intramolecular conformational rearrangements are allowed to occur during MD. For any assigned torsion value, the molecule was allowed to adjust its conformation over 5 ps of molecular dynamics simulations. Consequently, the occurrence of such conformational rearrangements accounts for the resulting rugged-like energy profiles depicted in Figure 1. For all model compounds, low-energy conformations have been selected from that systematic search approach in order to provide structural rationales for the discussion of the preferred reaction pathways. For that purpose, the extracted conformers are characterized by the benzophenone C═O oxygen-furanose-3′ and -4′ hydrogen distances as a structural parameter being diagnostic for a preorganized conformation, relevant for one of the two hydrogen-abstraction mechanisms.

However, it should be emphasized that the energetic differences between distinct minima of the energy profiles turned out to be in the range of a few kcal·mol$^{-1}$, thus rendering a clear discrimination among conformers somewhat difficult. The assumptions underlying the force field simulation such as neglecting any conformation-dependent stereoelectronic effects as well as the global treatment of the solvent environment may result in a less-pronounced discrimination among the energetic minima.

**Dihydroxy Model Compound 1.** The dihydroxy compound **1** displays three energetic minima within a range of 5 kcal·mol$^{-1}$ (Figure 1, **1A**−**C**). These three minima correspond to the two geometries required for 3′- (**1A**) and 4′-H-abstraction (**1B**,**C**), respectively. Of the three conformations, the one lowest in energy (**1C**) is preorganized for 4′-hydrogen abstraction. This particular conformation is stabilized by a hydrogen bonding network involving the two hydroxyl groups and the carbonyl oxygen atom of the carbonyl moiety, which should be particularly pronounced in the benzene solvent used for photolysis.

**Cyclic Carbonate 2.** The energetic minimum of the cyclic carbonate **2** (**2C**, Figure 1) corresponds to the conformation required for 4′-hydrogen abstraction. In the minimum **2B** found in our calculations, the carbonyl group of the benzophenone moiety is oriented away from both the 3′- and the 4′-hydrogen atoms. Thus, **2B** is believed to be photochemically inactive. Also in the third minimum conformer (**2A**, Figure 1), the orientation of the carbonyl group and the C−H-bonds in question is far from an optimal arrangement for homolytic C−H-bond fission.

**Dimethoxy Model Compound 3.** In the case of the dimethoxy model compound **3**, the minimum conformation **3A** (Figure 1) is ideally preorganized for 3′-H-abstraction. This is in clear contrast to the cases of **1** and **2** considered so far. The second minimum found for **3** (**3B**, Figure 1) is a conformation in which 4′-hydrogen abstraction is possible. Close examination of the conformation **3B** reveals an attractive interaction between the 3′-$OCH_3$ group and the distal phenyl ring of the benzophenone moiety, thus contributing to an intramolecular stabilization of that particular conformation. Due to the fact that these simulations were carried out without explicit treatment of a solvent environment, the importance of this van der Waals contact may be overemphasized.

**Dimesyloxy Model Compound 4.** Again, two minimum conformations were found: **4B** (Figure 1) is preorganized for 4′-H-abstraction, whereas the carbonyl group in **4A** is located such that 3′-H-abstraction may occur. Compared to the previously discussed simulations, the energy profile of **4** appears somewhat more pronounced, due to the steric bulk of the furanose substituents. Similar to the results obtained in the case of **3**, the conformation **4B** is stabilized by a van der Waals interaction between the distal benzene ring of the benzophenone moiety and the C3′ substituent. As discussed above for compound **3**, the energetic contribution of this interaction may in reality be less important than in the modeling. As a consequence, the energetic difference between the minima **4A** and **4B** may even be smaller.

## Discussion

The photochemistry of the four 4′-benzophenone-substituted nucleoside analogues **1**−**4** was studied. Five different photoproducts (**5**−**9**) were isolated and characterized. As diverse as these structures may seem at first glance, their formation can uniformly be explained by competing $\gamma$-H-abtraction/formation of photoenols, and $\delta$-H-abstraction. The purpose of the following discussion is to explain the partitioning of the two pathways as a function of the 2′,3′-substituents. As it turned out, the conformational analysis of **1**−**4** allows for a consistent rationalization of the observed effects.

**$\gamma$-H-Abstraction.** The product spectrum observed from the bis-hydroxy compound **1** and the cyclic carbonate **2** clearly points to photoenol formation as the common

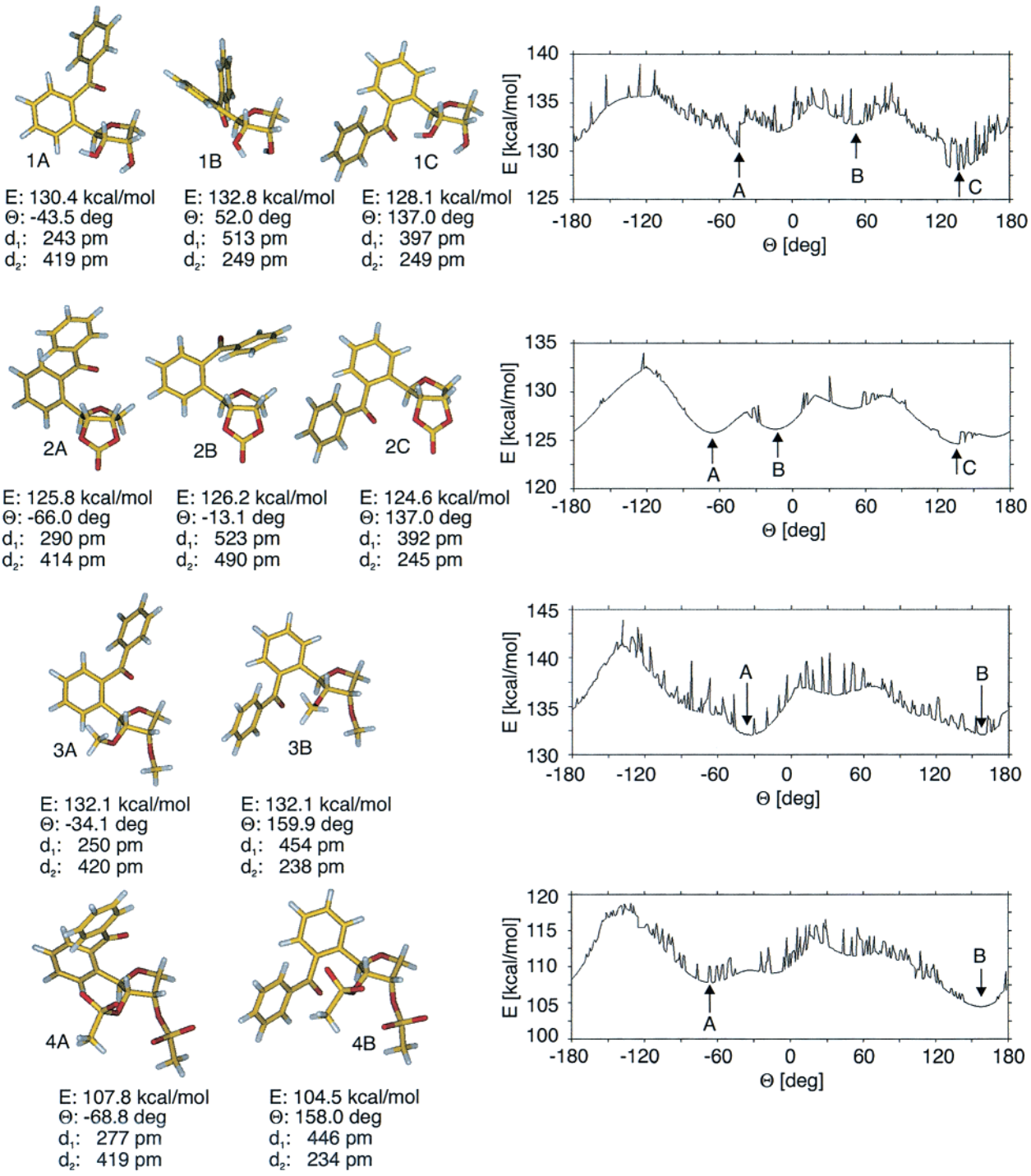


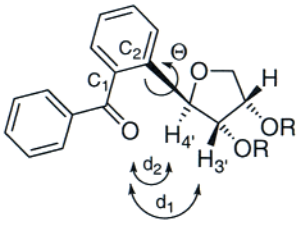


Θ: dihedral angle O-$C_{4'}$-$C_2$-$C_1$
$d_1$: distance C=O - $H_{3'}$
$d_2$: distance C=O - $H_{4'}$

**Figure 1.** Left: Selected low-energy conformations of compounds **1**−**4**, taken from the dynamic forcing simulation, shown in a stick mode. Carbon atoms are shown in yellow, hydrogen in white, and oxygen in red. Right: Energy profile for a full rotation around the bond connecting the benzophenone and the furan moiety.

and dominant photoreaction.[22] For example, the epimer **7** was isolated from the photolyzate of the cyclic carbonate **2**. Similarly, the dihydroxy compound **1** has to epimerize before ketal formation affording **5** can take place (Scheme 2). It appears reasonable to assume that the epimers **1**/**18** and **2**/**7** are in photoequilibrium.[23]

**Scheme 2**

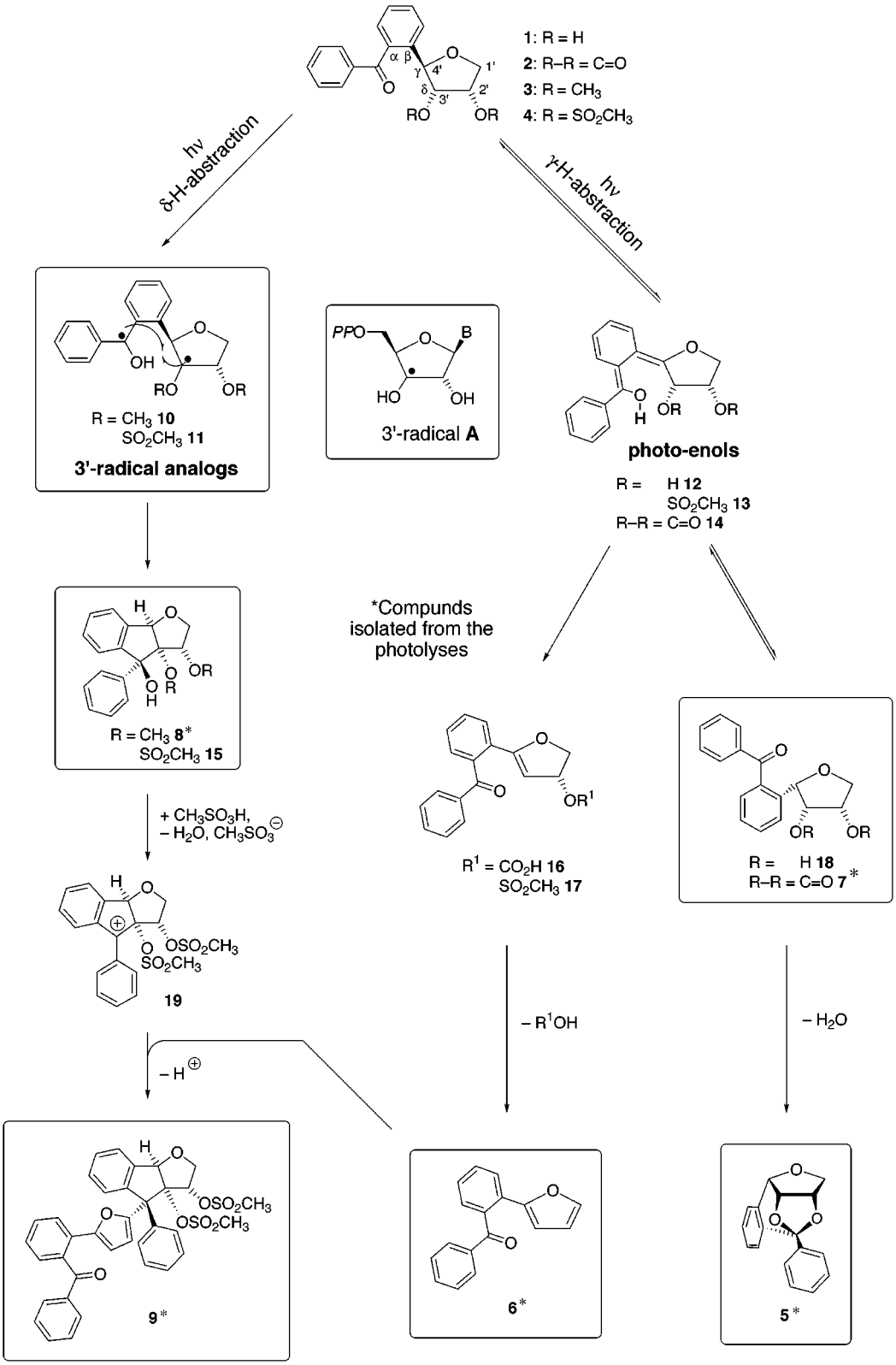


However, once the tricycle **5** is formed by intramolecular ketalization, the molecule is deprived of its chromophore. Thus, the formation of **5** becomes irreversible. Not unexpectedly, the tricyclic product **5** contained deuterium in the γ-position when the photolysis of **1** was carried out in the presence of deuterated acetic acid. γ-Protonation of the intermediate dienol **12** most likely accounts for the observed isotope exchange. Although seemingly different, also the formation of the furan **6** from the cyclic carbonate **2** can be explained by a closely related mechanism, again originating at the photoenol (**14**, Scheme 2). Since the carbonate moiety of **14** is a better leaving group than the 3′-hydroxyl of **12**, a new reaction channel

(22) The formation of photoenols is well established for *o*-alkylphenyl ketones, which do not undergo *Norrish-type* II cleavage. For reviews see ref 10a–c.

becomes available: 1,6-elimination from the dienologous hemiacetal **14** affords the unsaturated dihydrofuran **16**. The latter one aromatizes to the stable product **6**. It appears most likely that in the photoenols **13** and **14**, the 3′-oxygen atom is protonated by the acidic photoenol, and that subsequent elimination of mesylate (carbonate) gives rise to the dihydrofurans **16** and **17**. It is well-known that dihydrofurans of this type readily undergo further elimination to the aromatic furan system.[24,25] The preference of **1** and **2** for $\gamma$-H-abstraction can be rationalized by the preferential preorganization in their energetic minima (**1C**, **2C**, vide supra).

**$\delta$-H-Abstraction.** The dimethoxy compound **3** affords the tricycle **8** as the dominant photoproduct. The analogous formation of five-membered rings via cyclization of 1,5-biradicals, formed upon $\delta$-H-abstractions via seven-membered transition states, is well-known.[26] The $\delta$-H-abstraction which leads to the formation of 1,5-biradicals competes with the intrinsically favored $\gamma$-H-abstraction (1,4-biradical formation, six-membered transition state). The selectivity of radical $\gamma$-H- vs $\delta$-H-abstraction in triplet ketones was estimated to be ca. 20:1−15:1.[27] The predominant or exclusive formation of cyclization products via 1,5-biradicals is usually observed with ketones (i) lacking $\gamma$-hydrogen atoms,[29] (ii) having activated $\delta$-C−H bonds, e.g., $\delta$-alkoxyketones,[30] (iii) fixed conformations,[31] or (iv) with para-substituted benzophenones attached to rigid steroid systems. The latter arrangement was successfully used for the remote functionalization of the steroid skeleton.[32] In fact, unlike the cases of **1** and **2**, the minimum conformation of **3** favoring $\delta$-H-abstraction (**3A**, Figure 1) may be lower in energy, taking into account that the computational result for **3B** most likely includes an artificial stabilizing intramolecular interaction (vide supra). Thus, the conformational behavior of **3** accounts for the observed reactivity: In the cases of **1** and **2**, the conformations favoring $\delta$-H-abstraction are either not minima or are higher in energy compared to those preorganized for $\gamma$-H-abstraction. In contrast, the minimum **3A** found for **3** is ideally suited for 1,5-diradical formation (**10**, Scheme 2) and *not* higher in energy. In principle, the cyclization of the diradical **10** could give rise to four diastereomeric indeno[1,2-*b*]furans. However, the collapse of the 1,5-diradical derived from the minimum conformation **3A** (Figure 1) not only explains the constitution of the photoproduct **8**, but also the relative (and absolute) configuration of the newly formed stereogenic center at C-4. Finally, the preference of **3** for $\delta$- over $\gamma$-H-abstraction is further evidenced by the absence of deuterium incorporation at the benzylic carbon atom C-8b (see eq 5 for the atom numbering) when the photolysis was carried out in the presence of $CH_3CO_2D$.

Dimesyloxy model compound **4**: The photoproduct **9** combines the elements of the furan **6** and the tricycle **8** (Scheme 2). The most plausible pathway for the formation of the "dimer" **9** is the acid-catalyzed alkylation of the intermediate furan **6** by the tertiary alcohol **15** (via the benzhydrylic cation **19**, Scheme 2). The configuration of the benzhydrylic carbon atom of **9** reflects the *exo*-approach of the furan **6** on the concave cation **19** (Scheme 2). As mentioned in the case of **3**, formation of the tricycle (here compound **15**, Scheme 2) is best explained by the collapse of the 1,5-diradical **11**, derived from **4** by $\delta$-H-abstraction. However, the pathway leading to the furan **6** encompasses photoenol formation, i.e., $\gamma$-H-abstraction. Apparently, in the bis-mesylate **4**, the two competing pathways are followed simultaneously. Again, inspection of the minimum conformations **4A** and **4B** (Figure 1) supports this idea: Whereas **4A** should lead to $\delta$-H-abstraction, **4B** is well suited for photoenol formation. Since **4B** is somewhat lower in energy, a slight preference for photoenol formation may be expected. Whereas the furan **6** could actually be detected as an unstable intermediate in the photolysis of **4**, attempts to spectroscopically characterize the intermediate benzhydrylic alcohol **15** failed. Most likely, the acidic conditions of the photolysis prevent the accumulation of this material. It should finally be noted that in the present study, the C−O bond cleavage in the 2′-position was not yet observed. Instead, cyclization of the 1,5-diradicals **10** and **11** derived from the model compounds **3** and **4** (Scheme 2) occurred. Under the neutral (or in the presence of $CH_3CO_2D$ even acidic) conditions used, this is not quite unexpected: The importance of general base-catalysis for the elimination of the 2′-substituent from 3′-radicals has recently been shown by Giese et al.[9] In the active site of *E. coli* RNR, a glutamate residue most likely effects this catalysis.[8a,9] Consequently, further studies should include external or preferentially internal functional groups that effect the desired acid−base catalysis.

## Conclusion

4′-Benzophenone-substituted nucleoside derivatives were shown to undergo homolytic 3′-hydrogen abstraction, thus acting as functional models of the first step in the proposed mechanism of ribonucleotide reductases. The important aspect of 3′-radical formation by homolytic hydrogen abstraction was achieved. Our model system should thus prove useful in subsequent studies aiming at the elucidation of the following steps in the reaction mechanism of ribonucleotide reductases.

## Experimental Section

**General Methods. Experimental.** Unless otherwise noted, all reagents were purchased from commercial sources and were used as received. Benzene was distilled from and stored over sodium. Acetonitrile was distilled from $CaH_2$**.** Photoreactions

(23) See ref 10a.

(24) Similar reactions were observed with (i) acetylated C-glycosides with the benzylic 1′-position upon reaction with NBS and dibenzoyl peroxide, presumable via a benzylic radical in 1′-position: (a) Farr, R. N.; Kwok, D.-I.; Daves, G. D., Jr. *J. Org. Chem.* **1992**, *57*, 2093. (ii) with benzoylated C-glycosides having C−H acidic 1′-positions under acidic or basic conditions. Under basic conditions the dihydrofuran derivative was isolated. Acid treatment leads to elimination of the second benzoyl substituent and the formation of the furan system: (b) acidic conditions: Maeba, I.; Kitaori, K.; Ito, C. *J. Org. Chem.* **1989**, *54*, 3927. (c) basic conditions: Maeba, I.; Suzuki, M.; Hara, O.; Takeuchi; T.; Iijimar, T.; Furukawa, H. *J. Org. Chem.* **1987**, *52*, 4521.

(25) Depending on their substitution pattern, dihydrofurans very readily form furans. 4-Substituted 4,5-dihydrofurans with an α-proton in *anti*-position are especially labile. Altenbach, H. J.; Wolf, E. *Tetrahedron Asymmetry* **1993**, *4*, 2155.

(26) Wagner, P. J. *Acc. Chem. Res.* **1989**, *22*, 83 and ref 10a.

(27) Wagner, P. J.; Zepp, R. G. *J. Am. Chem. Soc.* **1971**, *93*, 4958. With alkoxy radicals $\gamma/\delta$-H-abstraction selectivities of 15:1 were found (see ref. 28).

(28) Walling, C.; Padwa, A. *J. Am. Chem. Soc.* **1963**, *85*, 1597.

(29) (a) Kraus, G. A.; Chen, L. *J. Am. Chem. Soc.* **1990**, *112*, 3464. (b) Wagner, P. J.; Meador, M. A., Park, B.-S. *J. Am. Chem. Soc.* **1990**, *112*, 5199. (c) Wagner, P. J.; Giri, B. P.; Scaiano, J. C.; Ward, D. L.; Gabe, E., Lee, F. L. *J. Am. Chem. Soc.* **1985**, *107*, 5483. (d) Wagner, P. J.; Kelso, P. A.; Kemppainen, A. E.; Zepp, R. G. *J. Am. Chem. Soc.* **1972**, *94*, 7500.

(30) Ounsworth, J.; Scheffer, J. R. *J. Chem. Soc., Chem. Commun.* **1986**, 232 and ref 29a.

(31) Paquette, L. A.; Balogh, D. W. *J. Am. Chem. Soc.* **1982**, *104*, 774.

(32) (a) Breslow, R. *Acc. Chem. Res.* **1980**, *13*, 170. (b) Breslow, R.; Baldwin, S.; Flechtner, T.; Kalicky, P.; Liu, S.; Washburn, W. *J. Am. Chem. Soc.* **1973**, *95*, 3251.

were carried out at ca. 20 °C with a Rayonet RPR-100 photoreactor using Duran vessels with internal water cooling. Solvents for photolysis were purged with dried Argon (99.98%). Flash chromatography was carried out on *E. Merck* or *Macherey-Nagel* silica gel 60 (230−400 mesh). For radial chromatography *E. Merck* silica gel 60 $PF_{254}$ with gypsum was used. Preparative HPLC was performed on an *E. Merck* LiChrosorb 100 RP-18, 10 $\mu$m column (250 × 50 mm) at a flow rate of 78 mL/min. For analytical HPLC a *Hewlett-Packard* LiChrospher 100 RP-18, 5 $\mu$m column (250 × 4 mm) was used. Chromatographic separations were conducted at 25 °C with a flow rate of 0.7 mL/min and the following linear gradients. Gradient 1: 0 min MeCN/$H_2O$ 30:70; 25 min MeCN/$H_2O$ 75:25, 27 min MeCN/$H_2O$ 100:0, 35 min MeCN/$H_2O$ 100:0; Gradient 2: 0 min MeCN/$H_2O$ 25:75; 25 min MeCN/$H_2O$ 75:25, 27 min MeCN/$H_2O$ 100:0, 35 min MeCN/$H_2O$ 100:0; Gradient 3: 0 min MeCN/$H_2O$ 40:60; 40 min MeCN/$H_2O$ 75:25, 42 min MeCN/$H_2O$ 100:0, 60 min MeCN/$H_2O$ 100:0.

**Computational Methods**. All molecular modeling studies and molecular mechanics simulations were carried out on Silicon Graphics Indigo2, O2, and Power Challenge computers. For interactive modeling and graphical display, the program Insight II (Biosym/MSI, San Diego, CA) was employed. All energy minimizations or molecular dynamics simulations were performed within the CFF91 force field[33] as implemented in the Discover program package, Version 2.95, using a dielectric constant of $\epsilon = 2$ accounting for the physicochemical characteristics of benzene. Within all molecular dynamics simulations, a time step of 1 fs was used for numerical integration of Newton's equation of motion by the Verlet algorithm.[34] The initial velocities were taken from a Maxwellian distribution resembling the desired target temperature. All compounds analyzed were manually constructed from fragments extracted from the Insight II fragment library and subsequently minimized interactively using either the steepest descent, or the conjugate gradient minimization, respectively.[35,36] The systematic search calculations utilized a dynamic forcing protocol in which the target value for the rotor torsion was systematically varied in 1 degree steps, in that a penalty term is added to the physical force field constraining the affected dihedral angle to the target value. The torsion forcing term was scaled by a harmonic force constant $k_\theta = 250$ kcal·mol$^{-1}$·rad$^{-2}$. For each of the 360 assigned rotational states of the systematically varied torsion, the structure was minimized for 100 iterations (conjugate gradients), subsequently initialized at a temperature of 300 K over 0.1 ps, followed by a 5 ps dynamics run, and finally energetically relaxed by 1000 steps of conjugate gradient minimization. Over the entire procedure the affected torsion was constrained harmonically to the corresponding target values. The resulting 360 conformers represent a full rotation around the dihedral angle of interest.

The principally available conformational space was explored by an elaborated combination of high energy molecular dynamics simulation with a simulated annealing procedure. After initialization at 10 K for 1 ps, the molecule was heated to a target temperature of 1000 K over a period of 24 ps, applying a weak temperature bath coupling scaled by an exponential decay constant of $\tau_T = 2$ ps. Over a production period of 1 ns at 1000 K, 500 snapshots were stored, each of which was subjected to a simulated annealing protocol, consisting of a cooling period of 5 ps to reach the final temperature of 300 K. Thus, the resulting conformational ensemble consists of 500 energetically relaxed structures, obtained by a smooth cooling procedure from the corresponding high energy snapshots.

**Photolysis of [2*R*-(2α,3*β*,4*β*)]-Phenyl[2-(tetrahydro-3,4-dihydroxy-2-furanyl)phenyl]methanone (1).**

**(a) In Benzene-$d_6$.** In a dry NMR tube, 21 mg (74 $\mu$mol) of **1** was dissolved in 0.5 mL of benzene-$d_6$. After purging of the clear, colorless solution with argon, the first $^1$H NMR spectrum (300 MHz) was recorded. The sample was irradiated four times at 350 nm: 1, 10, 25, and 30 min. During each irradiation period, the solution turned yellow. The color vanished almost completely within minutes after irradiation. Following each irradiation period, a $^1$H NMR spectrum was recorded. After the four irradiation periods (66 min of irradiation time at 350 nm), the pale yellow, slightly turbid solution was filtered through RP-18 silica and concentrated. Preparative HPLC (MeOH/$H_2O$ 75:25) yielded 6 mg (31%) of **5** as a colorless, highly viscous oil.

**(b) In Benzene-$d_6$ + AcOD**. In a dry NMR tube, 20 mg (70 $\mu$mol) of **1** was dissolved in 0.5 mL of benzene-$d_6$. After recording an initial $^1$H NMR spectrum, 40.5 $\mu$L (702 $\mu$mol) of $CH_3COOD$ was added. The clear, colorless solution was purged with argon and irradiated six times at 350 nm (1, 10, 25, 30, 30, and 30 min). After each irradiation period, a $^1$H NMR spectrum was recorded. After a total of 126 min of irradiation time at 350 nm, a pale yellow, slightly turbid solution resulted.

**[3*S*-(3α,3a*β*,5α,9b*β*)]-3,3a,5,9b-Tetrahydro-5-phenyl-2*H*-3,5-epoxyfuro[3,2-*c*][2]-benzopyrane (5).** $^1$H NMR (400 MHz, $CDCl_3$) $\delta$ 3.60 (dddd, $J$ = 10.7, 2.6, 0.6, 0.5 Hz; 1H, 2-$H_{ReS}$), 4.17 (dd, $J$ = 10.7, 5.7 Hz; 1H, 2-$H_{SiS}$), 4.82 (dddd, $J$ = 5.6, 5.6, 2.6, 0.7 Hz; 1H, 3-H), 5.34 (ddd, $J$ = 6.3, 5.4, 0.4 Hz; 1H, 3a-H), 5.38 (d, $J$ = 6.3 Hz; 1H, 9b-H), 6.61 (dddd, $J$ = 7.7, 1.3, 0.5, 0.5 Hz; 1H, 6-H), 7.11 (ddd, $J$ = 7.7, 7.5, 1.3 Hz; 1H, 7-H), 7.34 (ddd, $J$ = 7.5, 7.5, 1.3 Hz; 1H, 8-H), 7.42−7.45 (m; 3H, aryl-H), 7.49 (dddd, $J$ = 7.6, 1.3 Hz; 1H, 9-H), 7.60−7.64 (m; 2H, aryl-H); $^{13}$C NMR (75 MHz, $CDCl_3$) $\delta$ 71.5 (t), 74.1 (d), 78.8 (d), 79.6 (d), 107.9 (s), 124.5 (d), 126.6 (d), 127.6 (d), 128.0 (d), 128.8 (d), 129.0 (d), 129.8 (d), 132.5 (s), 137.3 (s), 142.8 (s); DQF-H,H-COSY (400 MHz, $CDCl_3$); JS-ROESY (400 MHz, $CDCl_3$): 230 ms mixing time, on-resonant pulses were used, 384 increments with 8 accumulations per increment and 2k complex points in $t_2$, zero-filling in both dimensions to 2k points, apodization with cos$^2$. Negative phased ROE correlations were obtained and integrated; IR (NaCl, film) 3068, 2972, 1082, 770, 698 cm$^{-1}$, TLC (EtOAc/hexane 8:2) $R_f$ 0.64; HRMS $m/z$ 266.0928 ($M^+$, 266.0943 calcd for $C_{17}H_{14}O_3$).

**Photolysis of [3a*R*-(3aα,4α,6aα)]-4-(2-Benzoylphenyl)-tetrahydrofuro-[3,4-*d*]-1,3-dioxol-2-one (2)**. A solution of 102 mg (329 $\mu$mol) of **2** in 355 mL of degassed, anhydrous benzene was irradiated under argon at 350 nm for 2 × 5 min. During each irradiation period, the solution turned from yellow to brown. The color vanished almost completely within minutes after irradiation. After each irradiation period, a sample was withdrawn and analyzed by HPLC (gradient 3). The photolysis was carried out up to 90% conversion. After a total of 10 min of photolysis, the clear, pale yellow solution was concentrated, affording 95 mg of a yellow oil. It was purified by preparative HPLC (MeOH/$H_2O$ 65:35), affording 37 mg (46%) of **6** as a yellow oil, 6 mg (6%) of **7**, and 9 mg (9%) **2** as colorless oils.

**[2-(2-Furanyl)phenyl]phenylmethanone (6).** $^1$H NMR (300 MHz, $CDCl_3$) $\delta$ 6.26 (dd, $J$ = 3.7, 1.8 Hz; 1H, 4-H), 6.42 (dd, $J$ = 3.7, 0.7 Hz; 1H, 3-H), 7.23 (dd, $J$ = 1.8, 0.7 Hz; 1H, 5-H), 7.33−7.41 (m; 4H, aryl-H), 7.47−7.56 (m; 2H, aryl-H), 7.71−7.78 (m; 3H, aryl-H); $^{13}$C NMR (75 MHz, $CDCl_3$) $\delta$ 108.7 (d), 111.5 (d), 126.6 (d), 127.4 (d), 128.2 (d), 128.3 (d), 129.0 (s), 129.6 (d), 129.9 (d), 133.0 (d), 136.9 (s), 137.1 (s), 142.6 (d), 151.7 (s), 198.7 (s); IR (NaCl, film) 1667, 759, 707 cm$^{-1}$; HPLC (gradient 3) $t_R$ = 32.3 min. HRMS (EI) $m/z$ 248.0861 ($M^+$, 248.0837 calcd for $C_{17}H_{12}O_2$)

**[3a*R*-(3aα,4*β*,6aα)]-4-(2-Benzoylphenyl)tetrahydrofuro-[3,4-*d*]-1,3-dioxol-2-one (7)**. $^1$H NMR (300 MHz, $CDCl_3$) $\delta$ 3.76 (dd, $J$ = 11.8, 3.5 Hz; 1H, 6-$H_a$), 4.43 (d, $J$ = 11.8 Hz; 1H, 6-$H_b$), 5.03 (d, $J$ = 3.5 Hz; 1H, 4-H), 5.26 (dd, $J$ = 6.8, 3.5 Hz; 1H, 3a- respectively 6a-H), 5.56 (dd, $J$ = 6.8, 3.5 Hz; 1H, 6a- respectively 3a-H), 7.38−7.51 (m; 4H, aryl-H), 7.59−7.65 (m; 2H, aryl-H), 7.76−7.84 (m; 3H, aryl-H); $^{13}$C NMR (75 MHz, $CDCl_3$) $\delta$ 72.0 (t), 80.6 (d), 81.5 (d), 81.8 (d), 127.4 (d), 128.5 (d), 128.8 (d), 130.3 (d), 130.4 (d), 131.8 (d), 133.3 (d), 135.6 (s), 137.7 (s), 154.2 (s), 197.9 (s); IR (NaCl, film) 1807, 1659,

(33) (a) Maple, J. R.; Dinur, U.; Hagler, A. T. *Proc. Natl. Acad. Sci. U.S.A.* **1988**, *85*, 5350. (b) Maple, J. R.; Thacher, T. S.; Dinur, U.; Hagler, A. T. *Chem. Des. Automat. News* **1990**, *5*, 5.
(34) Verlet, L. *Phys. Rev.* **1967**, *159*, 98
(35) Wiberg, K. B. *J. Am. Chem. Soc.* **1965**, *87*, 1070.
(36) Williams, J. E.; Stang, P. J.; Schleyer, P. v. R. *Annu. Rev. Phys. Chem.* **1968**, *19*, 531.

1163, 1091, 738, 703 $cm^{-1}$; HPLC (gradient 3): $t_R = 22.9$ min. HRMS (EI) 310.0861 ($M^+$, 310.0841 calcd for $C_{18}H_{14}O_5$)

**Photolysis of 2R−(2α,3*β*,4*β*)]-Phenyl[2-[tetrahydro-3,4-dimethoxy-2-furanyl]phenyl]methanone (3). (a) In Benzene.** A solution of 100 mg (320 μmol) of **3** in 355 mL of degassed, anhydrous benzene was irradiated five times under argon at 350 nm: 2, 6, 10, 12, and 10 min. During each irradiation period, the solution turned yellow. The color vanished almost completely within minutes after irradiation, at which time a sample was withdrawn and analyzed by HPLC (gradient 2). The photolysis was carried out until 100% conversion. After a total of 40 min of photolysis, the solvent was evaporated, affording 113 mg of a yellow oil. It was purified by preparative HPLC (MeOH/$H_2O$ 6:4), affording 40 mg (40%) of **8** as a pale yellow oil.

**(b) In Benzene-$d_6$.** In a dry NMR tube, 20 mg (64 μmol) of **3** was dissolved in 0.5 mL of benzene-$d_6$. After purging with argon, the first $^1$H NMR spectrum was recorded. The sample was then irradiated eight times at 350 nm for 1, 5, 10, 20, 34, 60, 67, and 120 min. During each irradiation period, the solution turned yellow. The color vanished almost completely within minutes after irradiation. Following each irradiation period, a $^1$H NMR spectrum was recorded. After a total of 317 min of irradiation, a pale yellow, clear solution resulted.

**(c) In Benzene-$d_6$** + AcOD. In a dry NMR tube, 20 mg (64 μmol) of **3** was dissolved in 0.5 mL of benzene-$d_6$. After recording an initial $^1$H NMR spectrum, 37 μL (642 μmol) of $CH_3COOD$ was added. The clear, colorless solution was purged with argon and irradiated eight times for 1, 5, 10, 20, 34, 60, 67, and 120 min. Following each irradiation period, a $^1$H NMR spectrum was recorded. After a total of 317 min a pale yellow, clear solution resulted.

**[3*S*-(3α,3aα,4*β*,8bα)]-3,3a,4,8b-Tetrahydro-3,3a-dimethoxy-4-phenyl-2*H*-indeno[1,2-*b*]furan-4-ole (8).** $^1$H NMR (300 MHz, $CDCl_3$) δ 3.18 (s; 3H, 16-$CH_3$), 3.35 (s; 1H, 4-OH), 3.43 (s; 3H, 15-$CH_3$), 3.97 (dd, $J$ = 8.8, 6.6 Hz; 1H, 2-$H_{ReS}$), 4.12 (dd, $J$ = 8.8, 7.0 Hz; 1H, 2-$H_{SiS}$), 4.36 (dd, $J$ = 7.0, 6.6 Hz; 1H, 3-H), 5.49 (s; 1H, 8b-H), 7.16−7.19 (m; 2H, 10,14-H), 7.22−7.29 (m; 4H, 5,11,12,13-H), 7.37−7.43 (m; 2H, 6,7-H), 7.46−7.49 (m; 1H, 8-H); (300 MHz, benzene-$d_6$) δ 3.35 (s; 1H, OH, exchange with $D_2O$), 3.17 (s; 3H, $OCH_3$), 3.32 (s; 3H, $OCH_3$), 3.93 (dd, $J$ = 9.4, 7.4 Hz; 1H, 2-$H_a$), 3.99 (dd, $J$ = 9.0, 6.1 Hz; 1H, 2-$H_b$), 4.29 (dd, $J$ = 7.4, 6.1 Hz; 1H, 3-H), 5.48 (s; 1H, 8b-H), 7.02−7.13 (m; 6H, aryl-H), 7.26−7.31 (m; 2H, aryl-H), 7.41−7.44 (m; 1H, aryl-H); $^{13}$C NMR (75 MHz, $CDCl_3$) δ 55.1 (q, C-16), 58.7 (q, C-15), 72.6 (t, C-2), 82.5 (d, C-3), 83.5 (d, C-8b), 85.5 (s, C-4), 96.0 (s, C-3a), 124.5 (d, C-5), 124.9 (d, C-8), 126.9 (d, C-10,14), 127.3 (d, C-12), 127.6 (d, C-11,13), 129.0 (d, C-7), 129.9 (d, C-6), 139.3 (s, C-8a), 142.9 (s, C-9), 145.4 (s, C-4a); E.COSY (400 MHz, 30 mg/0.3 mL $CDCl_3$) 90° pulse 7 μs, 384 increments with 36 accumulations per increment and 2k complex points in $t_2$, zero-filling in both dimensions to 2k points, apodization with $\sin^2$; JS-ROESY (400 MHz, 30 mg/0.3 mL $CDCl_3$) 320 ms mixing time, on-resonant pulses were used, 384 increments with 16 accumulations per increment and 2k complex points in $t_2$, zero-filling in both dimensions to 2k points, apodization with $\sin^2$. Negative phased ROE correlations were obtained and integrated; $^1$H,$^{13}$C-HMQC (400 MHz, 30 mg/0.3 mL $CDCl_3$) $^1$H: 90° pulse 7 μs, $^{13}$C: 90° pulse 16 μs, 512 increments with 20 accumulations per increment and 2k complex points in $t_2$, zero-filling in both dimensions to 2k points, apodization with $\sin^2$; $^1$H,$^{13}$C-HMBC (400 MHz, 30 mg/0.3 mL $CDCl_3$) $^1$H: 90° pulse 7 μs, $^{13}$C: 90° pulse 16 μs, 512 increments with 32 accumulations per increment and 2k complex points in $t_2$, zero-filling in both dimensions to 2k points, apodization with $\sin^2$; IR (KBr, pellet) 3462, 3387, 1130, 1118, 1071, 1034, 770, 702 $cm^{-1}$; HPLC (gradient 2): $t_R = 22.0$ min. MS (CI) $m/z$ (%) 313.0 [$(M + H)^+$]; HRMS (EI) $m/z$ 282.1222 ($(M - CH_2O)^+$, 282.1256 calcd for $C_{18}H_{18}O_3$).

**Photolysis of [2*R*-(2α,3*β*,4*β*)]-Phenyl[2-[tetrahydro-3,4-bis[(methylsulfonyl)oxy]-2-furanyl]phenyl]methanone (4).** A solution of 100 mg (227 μmol) of **4**, in 355 mL of degassed, anhydrous benzene, was irradiated five times under argon at 350 nm for 2, 5, 5, 10, and 10 min. During each irradiation period, the solution turned yellow. The color vanished almost completely within minutes after irradiation, at which time a sample was withdrawn and analyzed by HPLC (gradient 2). The photolysis was carried up to 96% conversion. After a total of 31 min photolysis, the clear, pale brown solution was concentrated, affording 95 mg of a brown-red oil. It was purified by preparative HPLC (MeOH/$H_2O$ 7:3), affording 12 mg (16%) of **9** as an orange oil and 4 mg (4%) of **4** as a yellow solid.

**[3*S*-3α,3aα,4α,8bα)]-Phenyl[2-[5-[3,3a,4,8b-tetrahydro-3,3a-bis[(methylsulfonyl)oxy]-4-phenyl-2*H*-indeno[1,2-*b*]-furan-4-yl]-2-furanyl]phenyl]methanone (9).** $^1$H NMR (300 MHz, $CDCl_3$; see Supporting Information pp S11, S12 for the atom numbering) δ 2.30 (s; 1H, 16-$CH_3$), 3.05 (s; 1H, 15-$CH_3$), 3.97 (ddd, $J$ = 10.7, 7.2, 0.8 Hz; 1H, 2-$H_{SiS}$), 4.23 (dd, $J$ = 10.7, 5.0 Hz; 1H, 2-$H_{ReS}$), 4.64 (ddd, $J$ = 7.2, 5.0, 0.6 Hz; 1H, 3-H), 6.02 (d, $J$ = 3.5 Hz; 1H, F3-H), 6.18 (d, $J$ = 3.5 Hz; 1H, F4-H), 6.70 (dd, $J$ = 0.8, 0.6 Hz; 1H, 8b-H), 7.07−7.10 (m; 1H, 5-H), 7.22 (ddd, $J$ = 7.6, 1.5, 0.6 Hz; 1H, B3-H), 7.26−7.52 (m; 11H, 6,7,8,11,12,13,B4,B5,B10,B11,B12-H), 7.55−7.58 (m; 2H, B9,-B13--H), 7.60−7.66 (m; 3H, 10,14,B6-H); $^{13}$C NMR (75 MHz, $CDCl_3$) δ 37.5 (q, C-16), 40.1 (q, C-15), 62.6 (s, C-4), 70.9 (t, C-2), 79.5 (d, C-3), 84.1 (d, C-4), 100.6 (s, C-3a), 110.0 (d, C-F4), 111.4 (d, C-F3), 125.6 (d, C-6), 126.9 (d, C-B6), 127.0 (d, C-5), 127.3 (d, C-B4), 127.9 (d, C-B3), 128.4 (d, C-B10,B12), 128.4 (s, C-B1), 128.6 (d, C-11,12,13), 129.1 (d, C-7,10,14), 129.6 (d, C-8H), 130.0 (d, C-B5,B9,B13), 133.2 (d, C-B11), 136.1 (s, C-9), 136.5 (s, C-B8), 136.7 (s, C-B2), 138.8 (s, C-8a), 139.4 (s, C-4a), 151.7 (s, C-F5), 155.7 (s, C-F2), 197.7 (s, C-B7); E.COSY(400 MHz, 9 mg/0.3 mL $CDCl_3$) 90° pulse 7 μs, 384 increments with 24 accumulations per increment and 2k complex points in $t_2$, zero-filling in both dimensions to 2k points, apodization with $\sin^2$; JS-ROESY (400 MHz, 9 mg/0.3 mL $CDCl_3$) 200 ms mixing time, on-resonant pulses were used, 384 increments with 32 accumulations per increment and 2k complex points in $t_2$, zero-filling in both dimensions to 2k points, apodization with $\sin^2$. Negative phased ROE correlations were obtained and integrated; $^1$H,$^{13}$C-HMQC (400 MHz, 9 mg/0.3 mL $CDCl_3$) $^1$H: 90° pulse 7 μs, $^{13}$C: 90° pulse 16 μs, 512 increments with 48 accumulations per increment and 2k complex points in $t_2$, zero-filling in both dimensions to 2k points, apodization with $\sin^2$; $^1$H,$^{13}$C-HMBC (400 MHz, 9 mg/0.3 mL $CDCl_3$) $^1$H: 90° pulse 7 μs, $^{13}$C: 90° pulse 16 μs, 512 increments with 80 accumulations per increment and 2k complex points in $t_2$, zero-filling in both dimensions to 2k points, apodization with $\sin^2$; IR (NaCl, film) 1668, 1411, 1361, 1180, 730 $cm^{-1}$; HPLC (gradient 2): $t_R$ = 33.2 min. MS (CI) $m/z$ (%) 671.6 [$(M + H)^+$]; HRMS (EI) $m/z$ 591.1481 ($(M - CH_3SO_2)^+$, 591.1477 calcd for $C_{35}H_{27}O_7S$).

**Acknowledgment.** The authors thank Prof. Dr. C. Griesinger and Dr. G. Zimmermann, Institut für Organische Chemie der Universität Frankfurt/Main, Germany, for supporting this work with NMR measurements. We gratefully acknowledge financial support from the Deutsche Forschungsgemeinschaft (priority program: "Novel reactions and mechanisms of catalysis in anaerobic microorganisms" grant nos. Be-998/4-1,2) and from the Fonds der Chemischen Industrie. T.E.L. thanks the Fonds der Chemischen Industrie for a Kekulé-fellowship.

**Supporting Information Available:** Time-dependent NMR monitoring of the photolyses of **1** and **3**. NMR analysis of the deuterium exchange experiment with **1**. Time-dependent HPLC monitoring of the photolyses of **2**−**4**. Coupling constants of eight tetrahydrofuro[3,4-*d*]dioxolanes with *trans*- and *cis*-orientated 4-substituents relative to the dioxolane ring. NMR data concerning the structure elucidation of compounds **5**, **8**, and **9**. Distance-distance plots (C═O−H3′/C═O−H4′) representing the 500 energetically relaxed structures obtained by the high-energy molecular dynamics simulation of **1**−**4** as well as their epimers. Energy profiles and low energy conformations of the dynamic forcing simulation of the 4′-epimers of **1**−**4**. This material is available free of charge via the Internet at http://pubs.acs.org.

JO991811S